Introduction

Thermal deformations are introduced in a structure when subjected to temperature changes. Human tooth structure in the oral environment is affected by considerable thermal fluctuations due to consumption of hot and cold fluids and food substances as well as heavy masticatory forces. Teeth are subjected to heavy occlusal stresses during normal function and parafunction. When occlusal forces are exerted on a tooth, stresses will be distributed throughout its structure. The clinical significance of this stress was first noted by McCoy.[1] Bending or flexing stresses will occur if the tooth is loaded eccentrically. As the tooth flexes, tensile and shear stresses are generated in the cervical region that cause disruption of the bonds between crystals of the glass-ceramic, leading to crack formation and eventual loss of the restoration.[2]

When a multiphase (composite) material such as a glass ceramic is subjected to thermal loading, the various constituents in it will respond differently, resulting in internal stresses and strains. These internal stresses and strains in glass ceramics may result in structural damages due to micro-cracking and interfacial debonding.[3]

Because glass-ceramics are brittle, strength testing of the material in the oral environments is difficult. Stress distributions as the result of an experimental load condition are complex and it is difficult to induce a pure compressive, tensile or shear stress in these environments.[4]

It has been reported that thermal changes together with the masticatory loads are able to create harmful stresses and initiate cracks within porcelains. For the understanding of postbonding cracks and internal thermal stress distribution, more information is required about the intimate structure of the tooth-restoration complex; and this analysis can be best performed with the well-accepted finite element (FEA) method modelling tool.[5]

In FEA method, basically, the object to be studied is graphically simulated in a computer in the form of a mesh, which defines the geometry of the body being studied. This mesh is divided, by a process known as discretization, into a number of sub-units termed elements. These are connected at a finite number of points called nodes, which are, in turn, defined by their global co-ordinates. The constituent elements are prescribed the appropriate material properties of the structure they represent. What is achieved is a mathematical model of the likely physical response of that object to load; large volumes of information on stresses, strains, and displacements being obtained through the continuum defined.[6-8]

The objective of this study was to analyze the stress distribution in a mandibular first premolar all ceramic crown cervical region under combined thermal and masticatory loading, by using a two-dimensional FEA and to evaluate the results of different all-ceramic crown materials with the natural tooth.

Materials and Methods

In this study, the following restorative materials were used: IPS Empress (IE), IPS Empress 2 (IE 2), Carrara press ceramic (Ca) and Ceramco FAC all-ceramic (Ce). Natural tooth (NT) structure was also included to compare the results. Variolink II (Ivoclar-Vivadent, Schaan, FL) dual-curing composite resin was used as the luting material (Table 1).

Table 1. Test materials.

Product	Code	Type	Manufacturer
IPS Empress	IE	Leucite-reinforced porcelain	Ivoclar-Vivadent, Schaan, FL
IPS Empress 2	IE 2	Lithia-based ceramic	Ivoclar-Vivadent, Schaan, FL
Carrara press ceramic	Ca	Leucite-reinforced ceramic	Elephant Dental Products- NL
Ceramco FAC all-ceramic	Ce	Lower leucite-reinforced ceramic	Ceramco, Burlington, NJ
Natural tooth structure	NT		

Models of axisymmetric 3-D structures may be represented in equivalent 2-D form. It can be expected that results from a 2-D axisymmetric analysis will be more accurate than those from an equivalent 3-D analysis. Because of total symmetry

about the z-axis as seen in Fig 1 all deformations and stresses are independent of the rotational angle. Thus, the problem needs to be considered as a two-dimensional problem. Therefore, two-dimensional finite element crown-mandibular first premolar tooth model with an intermediate cement layer in rounded shoulder preparation was designed for analysis of the stress distributions induced by applied thermal and masticatory loads for various all ceramic materials (Figure 1).[9] The tooth reduction finishing at the cement-enamel junction determined the dimensions of the all- ceramic crown (1 mm width at the cervical region, 1.5 mm occlusally and 1.2 mm buccolingually). The cement film thickness between the restoration and the dentine was taken as 25 µm. The anatomical shape of a buccolingual cross-section was digitized to trace the contour of enamel, dentin, and pulp chamber for the creation of a finite element model. The shapes and dimensions of the tooth, periodontal membrane, and alveolar bone were drawn from a past report.[10]

Figure 1. Three- dimensional finite element model (FEA) of tooth.

The 2D finite element model created by using ANSYS 5.4 (Swanson Analysis Systems Co., Houston, TX, U.S.A.) finite element software programme, was assumed to be isotropic, homogenous, elastic, axisymmetric and thermally solid which consisted of 11162 nodes and 10989 elements. Plane 75 type element was used as an axisymmetric ring element with a three-dimensional thermal conduction capability. The element has four nodes with a single degree of freedom temperature at each node. In order to determine the thermal stresses of the structure, the model was also analyzed structurally replacing the element by the equivalent structural element, Plane 25. Plane 25 is used for two dimensional modelling of axisymmetric structures with nonaxisymmetric loading. This element is defined by four nodes having three degrees of freedom per node and translations in the nodal x, y and z directions since the nodal points can move in three axes. The boundary conditions and loads are shown in Figure 1. As shown in the Figure, the model was fixed along the bone surface. A dense mesh modelling was performed on the prepared model. A finer mesh was generated at the material interface to ensure accuracy of temperature and masticatory load transfer.

The physical properties of enamel, dentine and all ceramic materials are given in Table 2.[11] The thermal properties of each ceramic material supplied by the manufacturers are presented in Table 3.[12] The thermal load application stages were determined assuming that each element was thermally balanced with the previous temperature after the thermal change occurred. The thermal load applied to the 2D tooth model having an initial temperature of 36°C simulated the draught of a cold (15°C) (T1) and a hot (60°C) (T2) liquid.[13,14] The hot and cold liquids were assumed to be held for 1 sec. in the mouth which means that the temperature of the oral cavity was thought to have reached 36°C in 1 sec.

After assigning thermal properties to the model and obtaining the thermal solutions, a total external load of 450 N (ML) was distributed over the nodes of the occlusal area for the simulation of combined thermal and masticatory loads. For the determination of the effects of masticatory forces alone, a load of 450 N was applied over the nodes of the occlusal area.

Table 2. Physical properties of the materials used in the study.

Material	Modulus of elasticity (MPa)	Poisson's ratio (v)
IPS Empress core material*	70000	0.25
IPS Empress layering material*	70000	0.25
IPS Empress 2 core material*	95000	0.25
IPS Empress 2 layering material*	60000	0.25
Carrara Press Core*	80000	0.25
Carrara Vincent*	71000	0.25
Ceramco PAC all-ceramic*	70000	0.19
Variolink II*	8300	0.24
Enamel+	48000	0.33
Dentine+	18600	0.31

(*) The physical properties of each material were supplied by the companies

(+) Farah *et al.*[11]

Table 3. Thermal properties of the materials used in the study

Material	Density (kg/mm^3)	Thermal expansion coefficient α (1/°C x10^{-6})	Thermal conductivity K (Calmm/mm^2 sn°C)x10-4	Specific heat c (Cal/kg°C)
IPS Empress core material*	2.40	17	3.50	233
IPS Empress layering material*	2.40	15	3.50	233
IPS Empress 2 core material*	2.40	10.60	3.50	233
IPS Empress 2 layering material*	2.40	9.70	3.50	23
Carrara Press Core*	2.60	14.70	2.67	238.70
Carrara Vincent*	2.40	14.70	2.14	262.59
Ceramco PAC all-ceramic*	2.41	13	2.52	195.27
Variolink II*	2.24	30	2.61	197
Enamel+	2.97	10	2.23	180
Dentine+	2.14	11.40	1.36	280

(*) All thermal data of the tested materials were obtained from the companies

(+) Phillips[12]

The thermal stresses in the tooth as a result of temperature changes and mastication induced stresses in the oral cavity were examined along the x-x axis. Since the stresses along the x-x axis had more critical values and the failure of a brittle material such as glass-ceramic, occurs when the obtained stresses have higher values, the maximal σ_y stresses were considered. The modified Von Mises criterion for brittle types of materials were also incorporated as this is the best predictor for crack formation.[5] Von Mises stresses demonstrated smaller values when compared with the maximum σ_y stresses along the x-x axis. Therefore, they were not included for stress evaluation. The stress patterns along the x-x axis were calculated at all nodal points of the line consisting of points A, B, C, D and E (Figure 2). These points were the critical points at which the temperature changes and the occurring stresses were maximum.

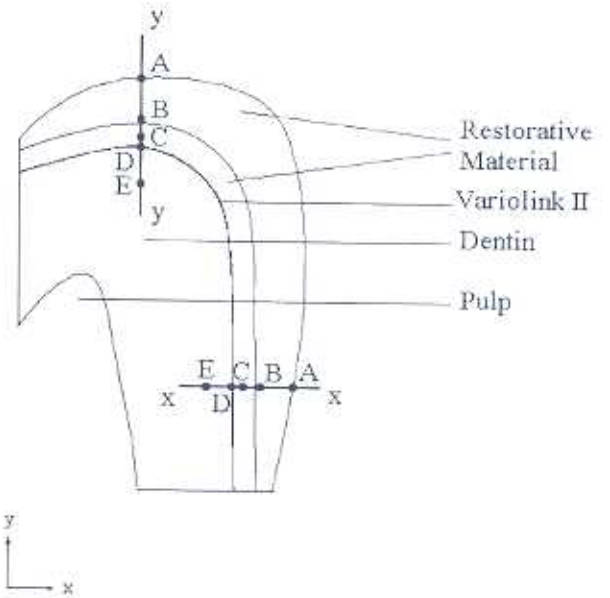

Figure 2. Calculated temparature and stress distributions at nodes A, B, C, D and E on the tooth.

Results

The stresses σ_x, σ_y and σ_z along the y-y axis exhibited similar characteristics in terms of distribution with the σ_x, σ_y and σ_y stresses along the x-x axis. Their similarities in stress distribution do not mean that they were equivalent in magnitude. The results revealed that maximum σ_y stresses

occurred along the x-x axis while maximum σ_x stresses along the y-y axis were observed.

The maximum temperature change was observed at the initial contact point (A) of the restorative material when 15°C cold (T1) or 60°C hot (T2) fluids were consumed. Temperature changes were recorded at points A, B, C and D reaching the normal oral cavity temperature 36°C between section D-E. Temperature related stresses were evaluated as sy stresses along the x-x axis. The stress values were compared as thermal changes (T1-T2), masticatory loads (ML) and their combination (T1-ML, T2-ML).

When T1 was applied on IE restorative material, a smaller tensile stress (0.4 MPa) was observed at point A changing into compressive stresses between section A-B. Compressive stresses occurred between B-C and C-D changing into tensile stresses between D-E region. The application of T1-ML created compressive stresses (4.9 MPa) at point A. While compressive stresses increased between A-B and B-C, a decrease was observed at point D. The compressive stresses increased between D-E. A maximum compressive stress (17.8 MPa) occurred at point A with the applied T2. While compressive stresses were recorded between A-B, the distribution of stresses between B-C were both compressive and tensile. The compressive stresses changed into tensile character at point D with a tensile stress distribution between section D-E. Compressive stresses (18 MPa) were recorded at point A with the applied T2-ML. The stress distributions between regions A-B, B-C and C-D were of compressive character changing into tensile stresses at point D. A compressive stress distribution was observed between D-E section (Figure 3).

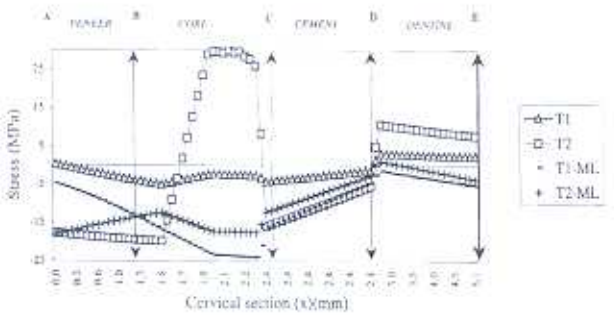

Figure 3. σ_y stresses for IE cervical region along the x-x axis (**T1:** 15°C, **T2:** 60°C, **ML:** Masticatory load)

The application of T1 to the IE 2 restorative material created a maximum tensile stress (3.9 MPa) at point A. The tensile stresses between A-B and B-C regions changed into compressive stresses between C-D with continous compressive stresses between D-E. When T1-ML were applied, compressive stresses (6.5 MPa) were recorded at point A. The stresses observed between A-B, B-C, C-D and D-E were compressive. The applied T2 load created compressive stresses (7.7 MPa) at point A. A compressive stress distribution was observed between A-B region. The compressive stresses changed into tensile stresses at point B with tensile stresses occurring between B-C region. The tensile stresses changed into compressive stresses between C-D region and the distribution between D-E was in a compressive pattern. The applied T2-ML created compressive stresses (18.9 MPa) at point A and distributed as compressive stresses between A-B, B-C, C-D and D-E (Figure 4).

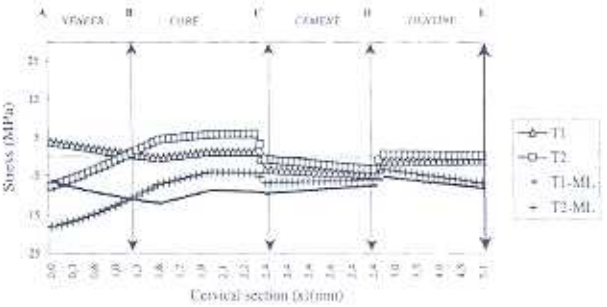

Figure 4. σ_y stresses for IE 2 cervical region along the x-x axis (**T1:** 15°C, **T2:** 60°C, **ML:** Masticatory load)

When T1 was applied to the Ca restorative material, tensile stresses (3.3 MPa) occurred at point A. The distributions between A-B, B-C, C-D and D-E were as compressive stresses. The applied T1-ML created compressive stresses (5.5 MPa) at point A. While increasing compresive stresses through A-B and B-C were observed, the compressive stresses through C-D and D-E regions decreased. With the application of T2, compressive stresses (11.8 MPa) were observed at point A. The decreasing compressive stresses through A-B region changed into tensile stresses at point B. The stress distribution at B-C region was in a tensile pattern. The compressive stresses observed at point C were in a compressive pattern through C-D region. The stresses changed

into tensile form at point D and distributed as tensile stresses through D-E region. The applied T2-ML created compressive stresses (19.7 MPa) at point A and distributed as compressive stresses through regions A-B, B-C, C-D and D-E (Figure 5).

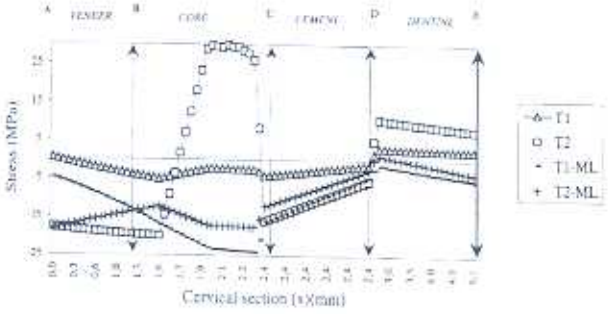

Figure 5. σ_y stresses for Ca cervical region along the x-x axis (**T1:** 15°C, **T2:** 60°C, **ML:** Masticatory load)

When T1 was applied to the Ce restorative material, tensile stresses (3.5 MPa) occurred at point A and were distributed between section A-B. While the tensile stresses changed into compressive stresses at point B, the distributions were as compressive stresses between B-C and C-D. The compressive stresses changed into tensile stresses at point D and were distributed as tensile stresses between D-E region. The applied T1-ML created compressive stresses (5.3 MPa) at point A. The stress distribution between A-B, B-C, C-D and D-E regions were in a compressive pattern. When T2 was applied, a compressive stress (9 MPa) was recorded at point A. The compressive stresses changed into tensile stresses at point B while a compressive stress distribution was observed between A-B. The tensile stresses changed into compressive stresses between C-D. The compressive stresses changed into tensile stresses at point D and distributed as tensile stresses between D-E region. The application of T2-ML created a maximum compressive stress (17.8 MPa) at point A. The distribution between A-B, B-C, C-D and D-E regions were as compressive stresses (Figure 6).

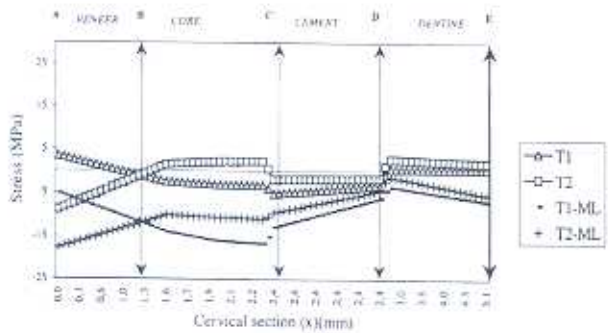

Figure 6. σ_y stresses for Ce cervical region along the x-x axis (**T1:** 15°C, **T2:** 60°C, **ML:** Masticatory load)

When T1 was applied at the initial contact point (A) of NT, maximum tensile stress (3.2 MPa) was observed. The decreasing tensile stresses between A-B, B-C and C-D sections changed into minimal compressive stresses between D-E region. When T1-ML were applied, compressive stresses (4.3 MPa) were recorded at point A. The increasing compressive stresses in all regions decreased between D-E region. When T2 was applied, compressive stresses (3.7 MPa) occurred at point A changing into tensile stresses at point B. B-C and C-D regions exhibited tensile stresses decreasing between D-E region. The application of T2-ML created increasing compressive stresses (11.2 MPa) at point A. A-B, B-C, C-D and D-E regions also exhibited compressive stresses (Figure 7).

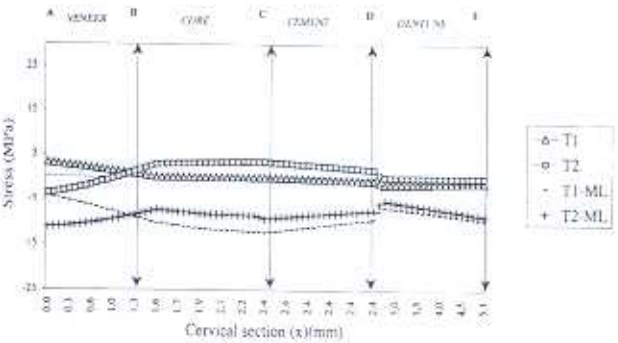

Figure 7. σ_y stresses for NT cervical region along the x-x axis (**T1:** 15°C, **T2:** 60°C, **ML:** Masticatory load)

Tensile stresses were recorded in all restorative materials and NT with the application of T1. The tensile stresses changed into compressive stresses when T1-ML were applied. The applied T2 created smaller compressive stresses compared with the compressive stress values occurred when T2-ML were applied. The obtained compressive stresses with the application of T2-ML were greater than the obtained compressive stresses when T1-ML were applied.

The application of masticatory loads on NT and restorative materials resulted in tensile stresses at point A. Mathematically similar tensile stresses turned into compressive stresses at A-B region. The stress distribution between regions B-C, C-D, D-E were of compressive character. The compressive stresses in NT were smaller in value compared with the restorative materials. The restorative materials exhibited similar stress patterns (Figure 8).

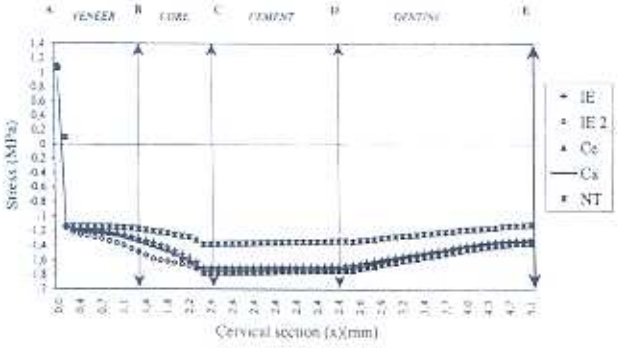

Figure 8. σ_y stress distributions of restorative materials and NT around cervical region under ML along the x-x axis.

The magnitude of the transition of compressive and tensile stresses is important for the resistance of a material to thermal and masticatory loads. The transition points are evaluated as critical regions.

Discussion

This study was done to calculate the maximum compressive and tensile stresses in the dentine, dentine-framework and framework-veneering material interfaces. The behaviour of all-ceramic materials under masticatory loads together with temperature changes were simulated and stress concentrations were determined to predict the potentially weakened areas of the tooth and restoration. To analyze the stress distribution in this FEA, the influence of the pulp chamber on the stress distribution was ignored, all materials were assumed to be linearly elastic and isotropic and they remained elastic under applied thermal and masticatory loads. The cement was assumed to bond perfectly to ceramic and dentine.[15,16]

Besides masticatory loads, thermal loads were also considered because the teeth are subjected to different temperatures of ingested food and drinks. Thermal records in the oral environment range between 0°C and 67°C,3 therefore the thermal loads were determined as 15°C (for cold liquids) and 60°C (for hot liquids) in this study because they were thought to be similar to the upper and lower boundries of thermal loads reported in literature.[3] Since enamel and dentine exhibit different physical and thermal properties, thermal loads may even create stresses in the intact natural tooth therefore the problem is amplified for the restored tooth.[17] The results of the present study also revealed that all tested all-ceramic systems exhibited different thermal and masticatory stresses when compared with each other and the natural tooth, but it is obvious that as the material properties approach to the natural tooth, the material creates less stresses on the restored tooth. The lithia-based all-ceramic material showed similar properties with NT in the present study. The thermal and masticatory stresses which occur in the restored tooth are dependent on many factors such as the properties of restorative materials, preparation design and adhesive resistance between tooth and restorative materials.[18] The present study included a FEA arranged to calculate node temperatures and the thermal, masticatory and their combined stress distribution in a restored tooth.[19,20]

In heat variations, the heat on the outer surface of the material can be lower or higher than the temperature of the environment. The reason for this is the transition of heat by convection to the outer surface. The heat transfer among the materials occurs via conduction. In this study, when a 60°C hot thermal load was applied, approximately a 7°C lower; and when a 15°C cold thermal load was applied, approximately a 12°C higher temperature were obtained at the initial contact point A in all tested all-ceramic materials. The results confirm the theoratical information about heat transfer. The temperature change at point E can be neglected when compared with the normal oral cavity temperature.

It has been reported that the fracture resistance decreases for all-ceramic crowns because of cyclic thermal and masticatory loading.[10] Saliva, thermal changes between 15°C and 45°C and masticatory

stresses in the oral cavity could also trigger and increase the all-ceramic crown fracture rate.[21]

The increase or decrease in temperature resulted in thermal stresses. The outer surface (point A) expanded because of the increase in temperature when a 60°C thermal load was applied. The inner surface (point E) showed less expansion since the increase in temperature was less according to the outer surface. Therefore, point E had a potential for blocking point A leading to the generation of tensile stresses at point E and compressive stresses at point A. Since the prepared model had a complex structure, combined compressive and tensile stresses occurred at the interfaces.[18]

When 60°C thermal load was applied together with the masticatory load, compressive stresses were observed, predominantly, while 15°C thermal load created tensile stresses on the restored tooth. When a 15°C thermal load was applied, tension at point A and compressive stresses at point E occured. Combined compressive-tensile stresses were present at the interfaces. The applied 15°C thermal load combined with the masticatory load resulted in stresses compressive in nature at point A, differing from the tensile stresses in the case of 15°C thermal load, alone.

For the resistance of the material, the areas of transition of compressive stresses to tensional stresses or tensional stresses to compressive stresses are critical points. The resultant stresses from 15°C thermal load together with the masticatory load were algebraically smaller than the compressive stresses obtained from 60°C thermal load combined with the masticatory load. These results might indicate that 15°C (or colder) thermal loading might create more harmful stresses for both tooth and restorative materials. The results revealed that, IE-2 ceramic material showed similar properties with NT. IE, Ce and Ca have greater stresses when compared with NT. The variety of thermal and mechanical loading results obtained from leucite based glass-ceramics, natural tooth and the lithia based glass-ceramic in the present study might be due to differences in ther mechanical properties such as their flexural strengths (leucite: 120-180 MPa, enamel: 65-75 MPa, dentin: 16-20 MPa and lithium disilicate: 340 MPa) that can be attributed to their different chemical compositions.[22]

A given thermal or masticatory load always has opposite effects on the restoration surface and the interface, increasing preexisting compressive stresses on one side and partially relieving them on the other.[3]

The design of tooth preparation, the mechanical properties (resistance to fracture, elastic modulus) of restorative materials, and bonding to dentin mechanisms should be in harmony to relieve the stresses induced by occlusal loads.

Conclusion

Within the limitations of this study, the following conclusions were drawn:

- Restorative materials were more affected from thermal and masticatory loads when compared with natural (intact) tooth.
- 15°C thermal loading created more stresses than 60°C thermal loading on the restorative materials tested in this study.

References

1. Mccoy G. The etiology of gingival erosion. *J Oral Implantol* 1982; 10: 361-362.
2. Lee WC, Eakle WS. Possible role of tensile stress in the etiology of cervical erosive lesions of teeth. *J Prosthet Dent* 1984; 52: 374-380.
3. Magne P, Douglas WH. Interdental design of porcelain veneers in the presence of composite fillings: finite element analysis of composite shrinkage and thermal stresses. *Int J Prosthodont* 2000; 13: 117-124.
4. Kelly JR, Tesk JA, Sorensen JA. Failure of all-ceramic fixed partial dentures in vitro and in vivo: analysis and modelling. *J Dent Res* 1995; 74: 1253-1258.
5. Korioth TW, Versluis A. Modeling the mechanical behavior of the jaws and their related structures by finite element (FE) analysis. *Crit Rev Oral Biology Medical* 1997; 8: 90-104.
6. Spears IR, van Noort R, Crompton RH, Cardew GE, Howard IC. The effects of enamel anisotropy on the distribution of stress in a tooth. *J Dent Res* 1993; 72: 1526-1531.

7. Van Noort R, Cardew GE, Howard IC, Noroozi S. The effect of local interfacial geometry on the measurement of the tensile bond strength to dentin. *J Dent Res* 1991; 70: 889-893.

8. Jones ML, Hickman J, Middleton J, Knox J, Volp C. A validated finite element method study of orthodontic tooth movement in the human subject. *J Orthod* 2001; 28: 29-38.

9. Wheeler RC. An atlas of tooth form. 2nd ed., W.B. Saunders Company, Philadelphia, USA, 1989, 64-66.

10. Nakamura T, Imanishi A, Kashima H, Ohyama T, Ishigaki S. Stress analysis of metal-free polymer crowns using the three-dimensional finite element method. *Int J Prosthodont* 2001; 14: 401-405.

11. Farah JW, Dennison JB, Powers JM. Effects of design on stress distribution of intracoronal gold restorations. *J Am Dent Assoc* 1977; 94: 1151-1154.

12. Phillips RW. Skinner's science of dental materials. 8th ed., W.B. Saunders Company, London, UK, 1982, 28-45.

13. Spierings TA, Peters MC, Bosman F, Plasschaert AJ. Verification of theoretical modeling of heat transmission in teeth by in vivo experiments. *J Dent Res* 1987; 66: 1336-1339.

14. Plant CG, Jones DW, Darvell BW. The heat evolved and temperatures attained during setting of restorative materials. *Br Dent J* 1974; 137: 233-238.

15. Anusavice KJ, Hojjatie B. Influence of incisal length of ceramic and loading orientation on stress distribution in ceramic crowns. *J Dent Res* 1988; 67: 1371-1375.

16. Rees JS. The effect of variation in occlusal loading on the development of abfraction lesion: a finite element study. *J Oral Rehabil* 2002; 29: 188-193.

17. Magne P, Versluis A, Douglas WH. Effect of luting composite shrinkage and thermal loads on the stress distribution in porcelain laminate veneers. *J Prosthet Dent* 1999; 81: 335-344.

18. Hood JA. Biomechanics of intact, prepared and restored tooth: some clinical implications. *Int J Prosthodont* 1991; 41: 25-32.

19. Brekelmans WA, Poort HW, Slooff TJ. A new method to analyse the mechanical behaviour of skeletal parts. *Acta Orthop Scand* 1972; 43: 301-317.

20. Hosey RR, Liu YK. A homeomorphic finite element model of the human head and neck. In: Finite elements in biomechanics (eds. RH Gallagher, BR Simon, PC Johnson JF Grossi, 3rd ed., John Willey, Johnson, New York, 1982, 379-402.

21. Palamara D, Palamara JE, Tyas MJ, Messer HH. Strain patterns in cervical enamel of teeth subjected to occlusal loading. *Dent Mater* 2000; 16: 412-419.

22. Ironside JG, Swain MV. Ceramics in dental restorations-A review and critical issues. *J Aust Ceram Soc* 1998; 34: 78-91.

Yazışma Adresi:

Dr. M. Ali GÜNGÖR

Ege Üniversitesi,
Dişhekimliği Fakültesi,
Protetik Diş Tedavisi AD,
35100 – Bornova / İZMİR
Faks : (232) 388 03 25
E-posta : maligungor@yahoo.com